



Research Article

A Bearing Fault Diagnosis Using a Support Vector Machine Optimised by the Self-Regulating Particle Swarm

Yerui Fan,¹ Chao Zhang ,^{1,2} Yu Xue,³ Jianguo Wang,^{1,2} and Fengshou Gu ⁴

¹School of Mechanical Engineering, University of Science and Technology of the Inner Mongol, Baotou 014010, China

²Inner Mongolia Key Laboratory of Intelligent Diagnosis and Control of Mechatronic Systems, Baotou, China

³Beijing Tianrun New Energy Investment Co., Ltd., Beijing 100000, China

⁴Department of Engineering and Technology, University of Huddersfield, Queensgate, Huddersfield HD1 3DH, UK

Correspondence should be addressed to Chao Zhang; zhanghero123@163.com

Received 4 October 2019; Revised 17 January 2020; Accepted 4 February 2020; Published 20 March 2020

Guest Editor: Seung-Yong Ok

Copyright © 2020 Yerui Fan et al. This is an open access article distributed under the Creative Commons Attribution License, which permits unrestricted use, distribution, and reproduction in any medium, provided the original work is properly cited.

In this paper, a novel model for fault detection of rolling bearing is proposed. It is based on a high-performance support vector machine (SVM) that is developed with a multifeature fusion and self-regulating particle swarm optimization (SRPSO). The fundamental of multikernel least square support vector machine (MK-LS-SVM) is overviewed to identify a classifier that allows multidimension features from empirical mode decomposition (EMD) to be fused with high generalization property. Then the multidimension parameters of the MK-LS-SVM are configured by the SRPSO for further performance improvement. Finally, the proposed model is evaluated through experiments and comparative studies. The results prove its effectiveness in detecting and classifying bearing faults.

1. Introduction

As a basic component, widely, rolling bearing is used in rotating machinery [1]. Rotating machinery is generally in the state of heavy work. Seriously, equipment performance is affected by bearing failure and even damaged [2]. Therefore, it is necessary to study the fault diagnosis of bearing. Intelligent diagnosis does not require people to wait beside the equipment that runs for a long time. It is suitable for monitoring areas that are in harsh environmental conditions, are sparsely populated, and are not suitable for long-term residential areas. Dong-yang Dou pointed out that, commonly, intelligent diagnostic methods include the K-Nearest Neighbor (KNN) algorithm, Probabilistic Neural Network (PNN), particle swarm optimization (PSO) optimized support vector machine (PSO-SVM), and a Rule-Based Method (RBM) based on the MLEM2 algorithm and a new Rule Reasoning Mechanism (RRM) [3]. RBM has the shortest time in the calculation process; relatively, the identification accuracy is low. It takes a long time in the training process of particle swarm optimization algorithm [3]. However, the PSO-SVM model takes a short time in the

recognition process, and the time spent in the training process is not concerned. Moreover, its recognition accuracy is high. In terms of fault diagnosis, the PSO-SVM model has a high accuracy which is satisfied by our requirements in the process of fault identification.

As shown in Figure 1, the fault identification accuracy of the support vector machine is mainly affected by the sample feature information and its parameters. The signal can be decomposed by empirical mode to obtain the intrinsic modal function (IMF). In terms of feature extraction, Chen et al. proposed that vibration signals could be decomposed by EMD to obtain the entropy of IMF as the feature vector [4]. Zhu et al. proposed that hierarchical entropy (HE) was calculated through multiscale entropy as the feature vectors [5]. The limitation of fault diagnosis is a single fault signal, and multifeature fusion information is richer [6]. Yu et al. proposed a fault diagnosis method based on multisensor information [7]. Multisensor signal acquisition is considered to be more comprehensive in perceptual cognition, but it is necessary to design the location of sensor installation. When a sensor is used to obtain the vibration signal of the bearing, it shall be installed as close to the bearing as possible. In

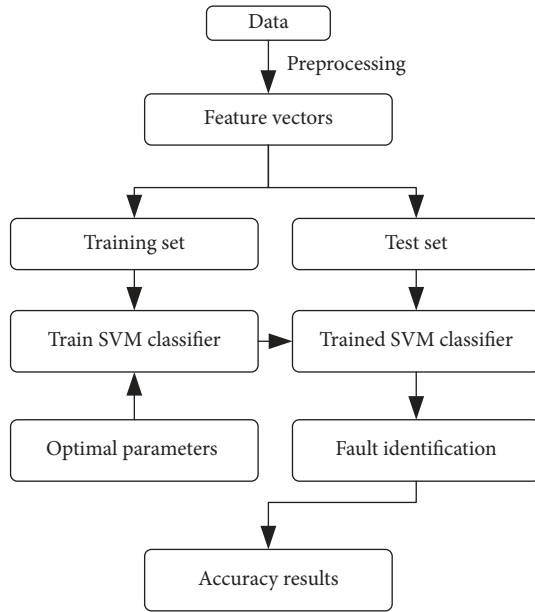


FIGURE 1: Flowchart of fault identification based on SVM.

general, for multisensor information fusion methods, it is considered very difficult to determine the location of each sensor. Xiang and Cen proposed an entropy fusion method based on kernel principal component analysis (KPCA). Firstly, the energy entropy of IMF and the singular entropy of IMF were obtained by EMD of the signal, and then the entropy value was fused by KPCA to obtain the feature vectors [6]. Compared with multiposition sensors, multi-entropy fusion can obtain comprehensive information without complicated sensor measurement system.

For rolling bearings, the speed varies slightly under different loads. Classification accuracy is what we care about. Generalization is required to provide better performance for SVM. In this paper, firstly, the energy entropy of IMF and the arrangement entropy of IMF are obtained through EMD theory in signal. Secondly, the feature matrix IMF's energy entropy and IMF's permutation entropy are fused through PCA to obtain the feature matrix. More comprehensively, the method can describe the bearing fault information, and it makes the SVM have better performance.

The classification accuracy of SVM is limited by kernel parameters, weights between different kernel functions, and penalty factors [8]. Traditional parameter optimization methods have poor convergence and cannot guarantee the maximum optimal solution, including trial and error, grid search, and gradient descent [9]. Zhang et al. proposed to optimize the SVM parameters by intercluster distance (ICD) in the feature space [9]. ICD combines grid search and multiple cross-validation. The method is cumbersome and the convergence is questionable in that Particle swarm optimization (PSO) algorithm is a kind of global random search optimization algorithm, which is easy to implement and has the advantages of low computation demands [10]. It is widely used for optimizing SVM [8, 11–13]. Zhu et al. optimized SVM by PSO [5]. Wu Deng optimized SVM by improved PSO [14]. In order to obtain better convergence

effect, Chen et al. proposed to optimize SVM parameters through chaotic PSO [4], which effectively improved the training process. However, due to the high degree of non-linearity involved in modeling multidimensional problems, there are still significant problems in obtaining efficient SVMs for fault identification.

LS-SVM is very suitable for solving small-sample, nonlinear, and high-dimensional problems. However, for solving nonlinear problems, in particular, the classification results of SVM are limited by the selection of kernel functions. Therefore, in order to verify the effectiveness of bearing diagnosis, a novel intelligent bearing diagnosis method is proposed by combining the advantages of empirical mode decomposition, multifeature, SRPSO algorithm, and least square support vector machine.

In this paper, the parameters of MK-LSSVM are optimized by the algorithm of SRPSO to obtain better performance. The fundamental of multikernel least square support vector machine (MK-LS-SVM) is overviewed to identify a classifier that allows multidimension features from empirical mode decomposition (EMD) to be fused with high generalization property. Then the multidimension parameters of the MK-LS-SVM are configured by the SRPSO for further performance improvement. Finally, the proposed model is evaluated through experiments and comparative studies. In the second section, different feature vectors, their fusion methods, and problems in LSSVM and their parameters are introduced. In the third part, the SRPSO algorithm is introduced, which includes the establishment of an objective function for fault identification. The fourth part is the fault diagnosis of the bearing. By fault diagnosis, this way, which is the SRPSO based multikernel LSSVM, is effectively proved to improve the accuracy. In the last section, the method is summarized.

2. Support Vector Machine Based Identification

2.1. Multikernel LSSVM. In fault diagnosis practice, it is usually difficult to obtain sufficient fault samples [5] for developing an intelligent system. Support vector machine can effectively classify small-samples and nonlinear signals and is widely used in mechanical fault identification [14]. The traditional classification recognition method is a combination of many binary classification support vector machines and requires large-scale training to learn [5]. Least square support vector machine (LS-SVM) based on statistical theory and minimal risk structure can be trained with less samples and avoid overfitting, with high generalization accuracy [5, 8, 11, 15]. The kernel of the polynomial kernel function in the kernel of the support vector machine has a strong generalization ability, but the learning ability is weak.

For rolling bearings, the values of speed may have a small difference under different loads. Classification accuracy is what we care about. Generalization is required to provide better performance for SVM. The Gaussian radial basis function kernel is a local kernel, and the learning ability is good, but the generalization ability is weak. Combining with the merits of these kernel functions allows a multikernel least square support vector machine (MK-LS-SVM) [10] to be developed. The

basic idea of the support vector machine is to classify the samples by nonlinear function space to high-dimensional spatial mapping so that the samples are classified according to different attributes [16], as shown in Figure 2.

Least squares support vector machine nonlinear estimation:

$$f(x) = \sum_{i=1}^n \alpha_i K(x, x_i) + b, \quad (1)$$

where $K(x, y)$ is a kernel function, b is an offset, and α_i is the weight.

Gaussian radial basis function kernel:

$$K_g = \exp\left(-g_k \cdot \|x - x_i\|^2\right). \quad (2)$$

The polynomial function kernel is defined as

$$K_d = (x^T x_i + 1)^{c_k}. \quad (3)$$

The resulting kernel function is obtained:

$$K = p_k \cdot (x^T x_i + 1)^{c_k} + (1 - p_k) \cdot \exp\left(-g_k \cdot \|x - x_i\|^2\right), \quad (4)$$

where p_k is the ratio of Gaussian kernel to polynomial kernel, c_k is the parameter for polynomial parameter kernel, and g_k is the Gaussian kernel parameter.

2.2. Selecting the Feature Vector of MK-LSSVM. Due to the different environmental conditions, the rolling bearing signal is nonlinear, nonstationary signal. Traditional time domain analysis and frequency domain analysis are mostly suitable for linear stationary signals [2, 4, 17], while empirical mode decomposition (EMD) is more suitable for nonlinear, nonstationary signal feature extraction [1, 18, 19]. The IMF's energy entropy and IMF's permutation entropy are obtained by EMD of bearing failure data.

(1) Let the signal be $x = \{x_1, x_2, \dots, x_n\}$

Permutation entropy reference [5]:

The m -dimensional vector delay of signal x_i :

$$x_i = \{x(i), x(i + \tau), \dots, x(i + (m - 1)\tau)\}, \quad (5)$$

where m is the embedded dimension and τ is the time delay. The c -dimensional delay of x_i is sorted in ascending order:

$$x_i = \{x(i + (k_1 - 1)\tau), x(i + (k_2 - 1)\tau), \dots, x(i + (k_m - 1)\tau)\}. \quad (6)$$

When $x(i + (k_{a-1} - 1)\tau) = x(i + (k_a - 1)\tau)$, take the order $k_{a-1} < k_a$.

The frequency of each arrangement is

$$p(h_k) = \frac{\text{Number}\{k | k \leq n - (m - 1)\tau, x_i^m \text{ has type } h\}}{n - (m - 1)\tau}. \quad (7)$$

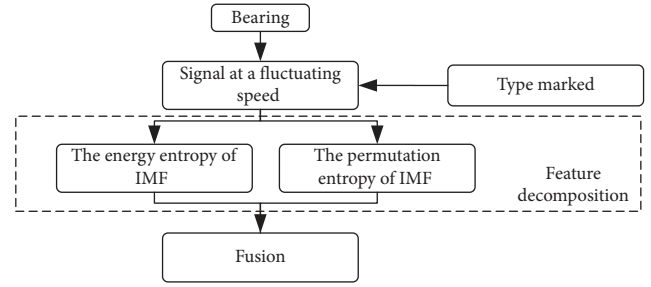


FIGURE 2: Bearing failure feature fusion.

Permutation entropy:

$$H_p(D) = - \sum_{h_k \in S_m} p(h_k) \ln(p(h_k)). \quad (8)$$

Energy entropy reference [18]:

The signal can be obtained by the empirical mode decomposition of the intrinsic modal function:

$$\text{IMF} = \{\text{imf}_1, \text{imf}_2, \dots, \text{imf}_n\}. \quad (9)$$

The energy of each intrinsic modal component imf_i is obtained:

$$E = \{E_1, E_2, \dots, E_n\}. \quad (10)$$

The sum of the energies of all intrinsic modal components:

$$E = \sum_{i=1}^n E_i. \quad (11)$$

Percentage of each intrinsic modal component:

$$p_i = \frac{E_i}{E}. \quad (12)$$

Energy entropy:

$$H_e = - \sum_{i=1}^n p_i \log p_i. \quad (13)$$

(2) Different speed will affect the bearing parts of the fault frequency and load changes. The entropy of the bearing under different rotational speeds is fused into the eigenvector. Feature fusion as shown in Figure 2 and its steps are as follows.

The energy entropy and permutation entropy of the IMF are obtained by decomposing the vibration signal through empirical mode

Mark the serial number of the different fault types

Use the fault type serial number to mark the fault feature

The fault feature and its corresponding markings at different rotational speeds are merged as fusion feature vectors

3. Self-Regulating PSO Optimized MKLS-SVM for Fault Identification

3.1. Self-Regulating PSO. The American social psychologist James Kennedy and electrical engineer Kennedy and Eberhart proposed the particle swarm optimization in 1995 [20]. The basic idea is to assume that there are groups of N particles in D -dimensional space, and the position and speed of each particle have been constantly updated.

The corresponding position of each particle i in the D -dimensional space:

$$X_i = (x_{i1}, x_{i2}, \dots, x_{iD}). \quad (14)$$

The corresponding velocity of each particle i in the D -dimensional space:

$$V_i = (v_{i1}, v_{i2}, \dots, v_{iD}), \quad (15)$$

where the speed of each particle will be based on its own t -generation previous speed (v_{id}^t), self-awareness ($c_1 r_1 (Pbest_i^t - x_{id}^t)$), and social awareness ($c_1 r_1 (Pbest_i^t - x_{id}^t)$) of three aspects of the update speed [21]. The velocity update of the i -th particle in the t -th generation in d dimension satisfies:

$$\begin{aligned} v_{id}^{t+1} = & \omega v_{id}^t + c_1 r_1 (Pbest_i^t - x_{id}^t) \\ & + c_2 r_2 (Gbest_g^t - x_{id}^t). \end{aligned} \quad (16)$$

The position update of the i -th particle in the t -th generation is satisfied:

$$x_{id}^{t+1} = x_{id}^t + v_{id}^{t+1}. \quad (17)$$

In addition to each particle history best position,

$$Pbest_i^t = (pbest_{i1}^t, pbest_{i2}^t, \dots, pbest_{iD}^t). \quad (18)$$

Particle history global best position:

$$Gbest^t = (Gbest_1^t, Gbest_2^t, \dots, Gbest_D^t). \quad (19)$$

Velocity range is $[v_{\min}, v_{\max}]$ and position range is $[x_{\min}, x_{\max}]$, where c_1, c_2 is the inertia weight. c_1, c_2 is the random number uniformly distributed between 2 $[0, 1]$. ω is the inertia weight, and the linear decreasing rate of each generation makes the convergence of the particle swarm optimization algorithm better [21]. $d = 1, 2, \dots, D$ represents the dimension of the particle.

Traditional particle swarm optimization algorithm because of the performance depends on the preset parameters and is therefore easy to fall into the local optimal [4]. In recent years, people can do this for the improvement can be divided into four categories: (a) based on the parameter setting algorithm, (b) based on neighborhood topology algorithm, (c) based on learning strategy algorithm, and (d) mixed type algorithm, which is based on learning strategies and mixed. Among them, the optimization of the type of algorithm is better [21]. As shown in Figure 3, based on the human cognitive psychology decision-making, the self-regulating particle swarm optimization algorithm introduces two strategies

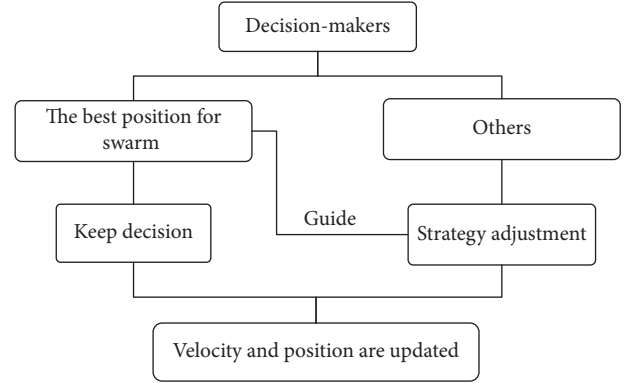


FIGURE 3: Human cognitive psychology optimal decision.

in the learning strategy. The first strategy is the setting of the inertia weight; that is, for the increase of the inertia weight of the optimal particles to accelerate the exploration of the optimal particles in the whole, and the rest of the particles are explored along the linearly decreasing inertia weight [21]. The second strategy is to select the search direction for the particles according to the self-cognition [21].

It is best for the particle to have the optimal search direction for its previous velocity direction and not to be influenced by self-cognition ($c_1 r_1 (Pbest_i^t - x_{id}^t)$) and social cognition ($c_1 r_1 (Pbest_i^t - x_{id}^t)$). Besides the direction of other particles' speed, the impact of self-cognition ($c_1 r_1 (Pbest_i^t - x_{id}^t)$) and social cognition ($c_1 r_1 (Pbest_i^t - x_{id}^t)$) on the speed has also to be considered. The ordinary particles are perceived by a uniformly distributed random number a of $[0, 1]$ to the global search direction. The ordinary particles will choose the social cognitive direction according to the uniform distribution random number a and the set threshold λ . If the uniform random number a reaches the threshold λ , it is considered that the social cognition is chosen; otherwise it is considered to abandon the social cognition. The size of the threshold λ has a certain screening effect on the choice of social cognition. From the point of view of probability, the greater the value of λ , the smaller the effect of social cognition on ordinary particles. The smaller the value of λ , the greater the effect of nonholonomic optimal particles on social cognition. That is, the logical value of the self-cognition and social cognitive part of the global optimal particle is 0; the logical value of the self-cognition part of the other particles is 1; the social cognitive part is the logical value of 1 when the uniform distribution random number a satisfies the threshold λ ; and the logic value is zero when λ is not satisfied.

3.2. Implementation Steps

- (1) Initialize the position and velocity of each particle.
- (2) Calculate the fitness value of each particle.
- (3) The initial particle position is set to the historical optimal position $Pbest$ and the $Pbest$ fitness value is

compared to obtain the initial historical global optimal position G_{best} .

- (4) Calculate the self-regulating inertia weight (w) of each particle.

For the best particles,

$$w = w + \eta * \Delta w. \quad (20)$$

Other particles:

$$w = w - \Delta w, \quad (21)$$

where Δw satisfies condition $\Delta w = (w_I - w_F)/N_{Iter}$. w_I is the initial value of the inertia weight. w_F is the inertia weight termination value. N_{Iter} is the number of iterations and η is a constant that controls the acceleration rate.

- (5) Update the particle velocity and position.

$$\text{Velocity update} \begin{cases} v = w * v, & \text{for best particle,} \\ v = w * v + c_1 * r_1 * (P_{best} - x) + c_2 * r_2 * P * (G_{best} - x), & \text{otherwise,} \end{cases} \quad (22)$$

where c_1, c_2 is the acceleration coefficient. r_1, r_2 is the random number in the range of (0, 1). P is the particle social cognition:

$$P = \begin{cases} 1, & \text{if } a > \lambda, \\ 0, & \text{otherwise,} \end{cases} \quad (23)$$

where a is a random number and λ is the set threshold, typically 0.5.

- (6) Calculate the particle fitness value after updating the position.
- (7) Update the best position of each particle and the global best position of the particle swarm.
- (8) To determine if the end of the conditions is not met, the conditions are returned 4).

In this paper, r_1, r_2 is the random number in the range of (0, 1); $c_1 = 1.49445$; $c_2 = 1.49445$; $\lambda = 0.5$.

3.3. The SRPSO Optimized MKLS-SVM Model. SRPSO optimization MKLS-SVM fault diagnosis process shown in Figure 4. From formula (8) we can see that there are three parameters in the multikernel least squares support vector machine. Difficulty: Gaussian radial basis function kernel g_k , polynomial function kernel parameter c_k , and weight p_k . The energy entropy and permutation entropy are obtained by empirical mode decomposition of the fault signals of bearings under different rotational speeds. The different entropy values at different rotational speeds are used as the eigenvectors of the signals for the training and testing of multikernel least squares support vector machines. SRPSO in CEC2005 for single-peak, basic multichannel, extended multichannel, and mixed type function test shows a better convergence [15]. The adaptive parameters of the multikernel support vector machine can be found by SRPSO. The appropriate parameters

can reduce the SVM classification error ratio. The ratio of the correct number of SVM fault classification and the number of sample signals under different parameters are taken as the fitness target of particle swarm optimization algorithm. The self-regulating PSO can optimize the SVM parameters and can be realized by optimizing the fitness function values in the training samples. Finally, the test samples are entered into the trained SVM, and the classification accuracy of the test samples can be obtained.

4. Fault Detection

In order to verify the effectiveness of the proposed method, the experimental data of the Electrical Engineering Laboratory at Case Western Reserve University were selected [22], which have been explored by many researchers. The tested bearing was a drive end bearing Type 6205-2RS.

4.1. Experimental Data. The sampling frequency is 12,000 Hz. Defect dimensions for bearings are 0.021", 0.014", 0.021", 0.028". For each original collected signal that represents one working condition, the first 120,000 points (the sampling time is 10 s) were divided into 50 subsignals. Each subsignal contains 2400 points (sampling time is 0.2 s). A set of signals is composed of all subsignals in different environments. A sample is randomly selected in the set of vibration signals in various environments, as shown in Figure 5. The IMF of this sample is calculated through EMD, as shown in Figure 6.

As shown in Figure 6, comparing with other IMF components, it can be seen that the amplitude of the 7th to 8th IMF component is very small. Therefore, taking the first six IMF components is enough to express the original signal. The entropy value of IMF was obtained through EMD. Some entropy values are listed below:

IMF's energy entropy, as shown in Tables 1–4:

IMF's permutation entropy, as shown in Tables 5–8.

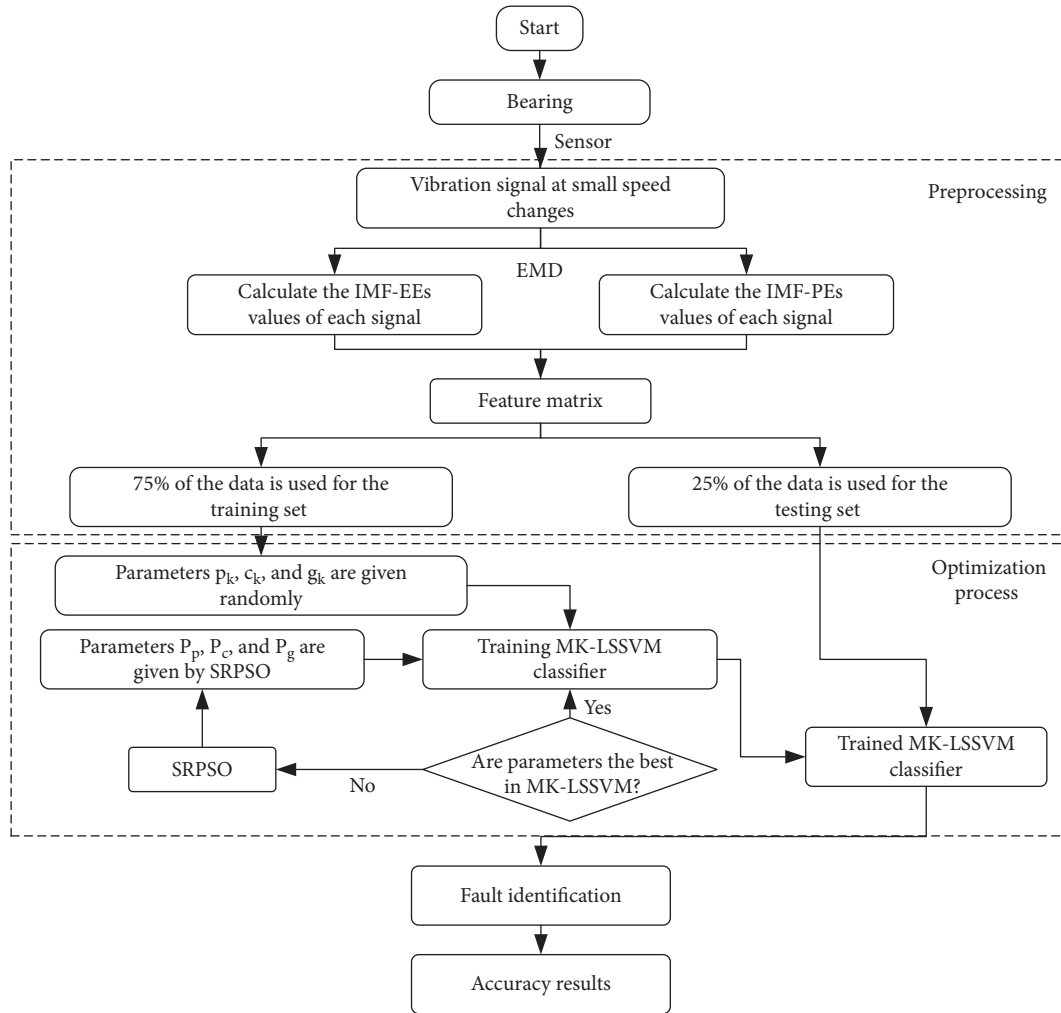


FIGURE 4: MKLS-SVM failure classification process.

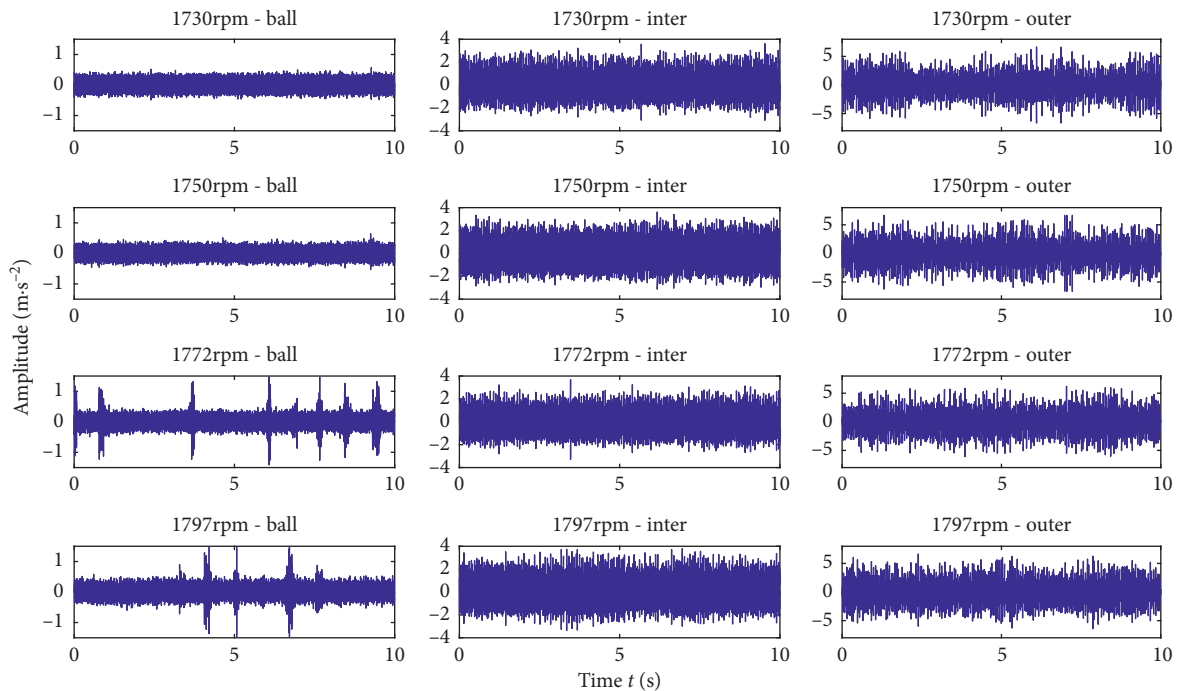


FIGURE 5: Bearing vibration signals in different environments.

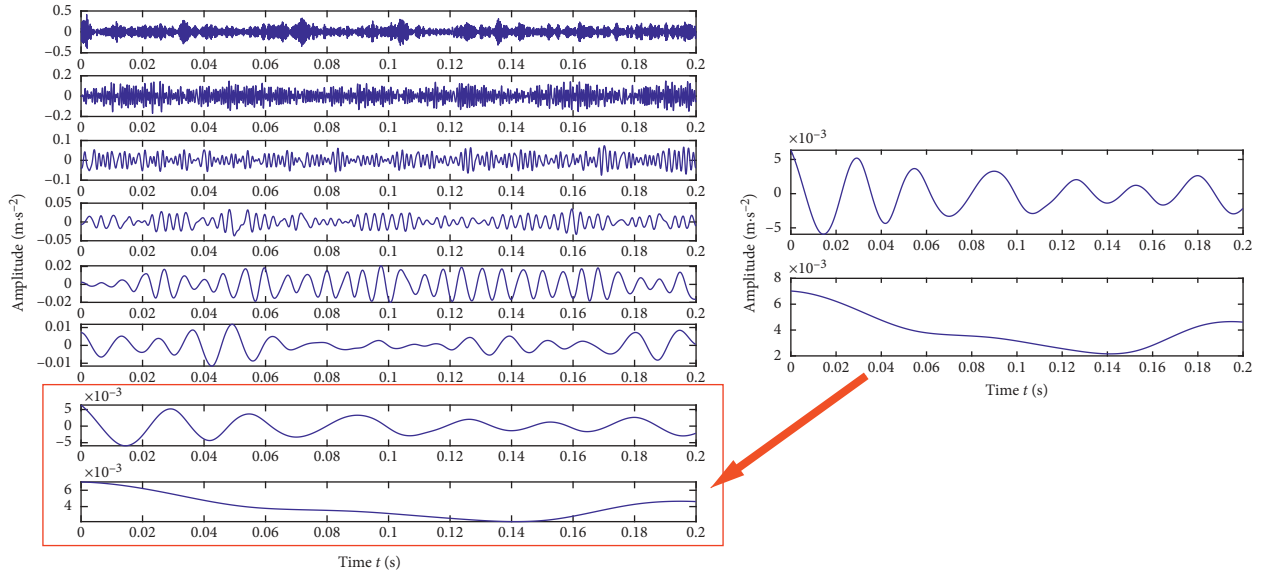


FIGURE 6: The IMF's of sample.

TABLE 1: Energy entropy at 1730 rpm.

Fault location	Fault mark	Feature number	Energy entropy at 1730 rpm					
			E_1/E	E_2/E	E_3/E	E_4/E	E_5/E	E_6/E
Inner ring	1	1	0.0007	0.1019	0.1359	0.0260	0.0158	0.0037
	1	2	0.0012	0.1102	0.1693	0.0306	0.0135	0.0032
	1	3	0.0008	0.0946	0.1475	0.0349	0.0146	0.0034
	1	4	0.0009	0.1166	0.1488	0.0274	0.0145	0.0047
	1	5	0.0005	0.0901	0.1214	0.0457	0.0097	0.0050
Outer ring	2	1	0.0028	0.2061	0.1835	0.0753	0.0258	0.0131
	2	2	0.0029	0.1865	0.2030	0.1029	0.0558	0.0128
	2	3	0.0023	0.1790	0.1838	0.0879	0.0269	0.0099
	2	4	0.0018	0.1587	0.1754	0.0672	0.0101	0.0095
	2	5	0.0023	0.1612	0.1939	0.1079	0.0189	0.0123
Ball	3	1	0.0694	0.5219	0.2552	0.0942	0.0645	0.0145
	3	2	0.0626	0.5171	0.2399	0.1127	0.0784	0.0121
	3	3	0.0710	0.5227	0.2569	0.1226	0.0879	0.0188
	3	4	0.0801	0.5266	0.2808	0.1494	0.1120	0.0059
	3	5	0.0846	0.5285	0.2663	0.1228	0.0894	0.0140

4.2. *Fault Detection.* The process of SVM classification is influenced by its parameters. Generally, PSO is used as a method to optimize parameters. To do this, we need to compare the performance of PSO and SRPSO. The parameters of LSSVM are optimized by PSO, as shown in Figure 7(a). The parameters of LSSVM are optimized by SRPSO, as shown in Figure 7(b).

Figures 7(a) and 7(b) show that SRPSO has a good convergence for optimization of SVM parameters, and no more than 6 generations can be obtained to obtain the optimal solution, thus, selecting the update of the sixth passage.

The study was divided into three parts:

- (a) How the eigenvectors are obtained has been given. Firstly, the EE and PE of each subsignal are obtained

through EMD, and then the entropy value is fused to form the eigenvector.

- (b) The model for fault identification has been obtained. The parameters of MK-LSSVM were optimized by SRPSO, and the theoretical model of MK-LSSVM to identify fault defects was constructed.
- (c) The defect of rolling bearing has been identified. The model is used for signal detection to complete the flaw detection of bearing signal.

In this paper, compared with other methods, the superiority of the proposed method is reflected. The first group is the method mentioned in the literature [5]. The second group is the method proposed in the literature [10]. The

TABLE 2: Energy entropy at 1750 rpm.

Fault location	Fault mark	Feature number	Energy entropy at 1750 rpm					
			E_1/E	E_2/E	E_3/E	E_4/E	E_5/E	E_6/E
Inner ring	1	1	0.0008	0.0763	0.1523	0.0355	0.0109	0.0027
	1	2	0.0007	0.0785	0.1475	0.0338	0.0105	0.0038
	1	3	0.0006	0.0727	0.1329	0.0412	0.0096	0.0046
	1	4	0.0006	0.0727	0.1399	0.0274	0.0130	0.0044
	1	5	0.0010	0.1108	0.1503	0.0837	0.0182	0.0090
Outer ring	2	1	0.0026	0.1709	0.2052	0.0809	0.0111	0.0024
	2	2	0.0033	0.1696	0.2349	0.0589	0.0202	0.0116
	2	3	0.0029	0.2007	0.1956	0.0616	0.0219	0.0118
	2	4	0.0050	0.2380	0.2187	0.1510	0.0445	0.0118
	2	5	0.0027	0.1926	0.2002	0.0465	0.0143	0.0063
Ball	3	1	0.0233	0.4209	0.2811	0.1723	0.0938	0.0065
	3	2	0.0176	0.3860	0.2891	0.1074	0.0965	0.0121
	3	3	0.0158	0.3736	0.2628	0.1848	0.1141	0.0233
	3	4	0.0184	0.3991	0.2535	0.1641	0.0982	0.0197
	3	5	0.0165	0.3694	0.3037	0.1283	0.0814	0.0314

TABLE 3: Energy entropy at 1772 rpm.

Fault location	Fault mark	Feature number	Energy entropy at 1772 rpm					
			E_1/E	E_2/E	E_3/E	E_4/E	E_5/E	E_6/E
Inner ring	1	1	0.0010	0.0844	0.1648	0.0456	0.0155	0.0052
	1	2	0.0011	0.1011	0.1650	0.0387	0.0112	0.0059
	1	3	0.0008	0.1129	0.1307	0.0729	0.0147	0.0068
	1	4	0.0007	0.0874	0.1410	0.0273	0.0097	0.0009
	1	5	0.0009	0.0942	0.1564	0.0338	0.0106	0.0014
Outer ring	2	1	0.0061	0.1713	0.2980	0.1059	0.0230	0.0086
	2	2	0.0059	0.2046	0.2863	0.0580	0.0251	0.0178
	2	3	0.0041	0.1942	0.2418	0.1045	0.0326	0.0136
	2	4	0.0041	0.1721	0.2573	0.0772	0.0126	0.0043
	2	5	0.0030	0.1285	0.2425	0.0610	0.0142	0.0088
Ball	3	1	0.0014	0.1433	0.1569	0.0792	0.0505	0.0140
	3	2	0.0038	0.2138	0.2023	0.1290	0.0856	0.0194
	3	3	0.0056	0.2081	0.2540	0.1703	0.0855	0.0218
	3	4	0.0011	0.1345	0.1370	0.0728	0.0536	0.0107
	3	5	0.0009	0.1411	0.1103	0.0671	0.0296	0.0113

TABLE 4: Energy entropy at 1792 rpm.

Fault location	Fault mark	Feature number	Energy entropy at 1792 rpm					
			E_1/E	E_2/E	E_3/E	E_4/E	E_5/E	E_6/E
Inner ring	1	1	0.0018	0.1077	0.2051	0.0478	0.0113	0.0049
	1	2	0.0024	0.1174	0.2244	0.0365	0.0095	0.0040
	1	3	0.0018	0.1049	0.1986	0.0983	0.0104	0.0034
	1	4	0.0021	0.1132	0.2166	0.0460	0.0068	0.0029
	1	5	0.0018	0.1247	0.1994	0.0565	0.0116	0.0034
Outer ring	2	1	0.0091	0.2671	0.2952	0.1591	0.0418	0.0198
	2	2	0.0045	0.1727	0.2660	0.0821	0.0393	0.0227
	2	3	0.0037	0.1649	0.2482	0.0673	0.0221	0.0130
	2	4	0.0037	0.1431	0.2415	0.1476	0.0328	0.0121
	2	5	0.0055	0.2264	0.1707	0.2395	0.0660	0.0168
Ball	3	1	0.0055	0.2555	0.2340	0.0789	0.0545	0.0093
	3	2	0.0075	0.2626	0.2810	0.0841	0.0428	0.0235
	3	3	0.0050	0.2552	0.2167	0.0825	0.0498	0.0205
	3	4	0.0085	0.2851	0.2799	0.0860	0.0456	0.0137
	3	5	0.0054	0.2305	0.2568	0.0858	0.0578	0.0142

TABLE 5: Permutation entropy at 1730 rpm.

Fault location	Fault mark	Feature number	Permutation entropy at 1730 rpm					
			PE_1	PE_2	PE_3	PE_4	PE_5	PE_6
Inner ring	1	1	0.7421	0.5522	0.3756	0.2768	0.2020	0.1605
	1	2	0.7502	0.5321	0.3656	0.2704	0.1943	0.1585
	1	3	0.7609	0.5692	0.3836	0.2811	0.2035	0.1592
	1	4	0.7531	0.5219	0.3538	0.2713	0.1896	0.1513
	1	5	0.7399	0.5158	0.3623	0.2923	0.2125	0.1662
Outer ring	2	1	0.8071	0.6348	0.4092	0.3008	0.2386	0.1830
	2	2	0.8112	0.6038	0.4010	0.3160	0.2720	0.2020
	2	3	0.8092	0.6609	0.4291	0.3104	0.2516	0.1925
	2	4	0.8039	0.6134	0.3875	0.3069	0.2239	0.1796
	2	5	0.8060	0.5603	0.3848	0.2961	0.2292	0.1864
Ball	3	1	0.8002	0.5068	0.3674	0.2595	0.1890	0.1512
	3	2	0.8222	0.5497	0.3853	0.2719	0.1948	0.1614
	3	3	0.8141	0.5333	0.3847	0.2752	0.1882	0.1447
	3	4	0.8083	0.5193	0.3939	0.2779	0.1920	0.1493
	3	5	0.8133	0.5223	0.3826	0.2764	0.1964	0.1580

TABLE 6: Permutation entropy at 1750 rpm.

Fault location	Fault mark	Feature number	Permutation entropy at 1750 rpm					
			PE_1	PE_2	PE_3	PE_4	PE_5	PE_6
Inner ring	1	1	0.7495	0.5696	0.3642	0.2677	0.1942	0.1593
	1	2	0.7450	0.5521	0.3716	0.2879	0.2047	0.1601
	1	3	0.7441	0.5945	0.3809	0.2838	0.2090	0.1696
	1	4	0.7461	0.5290	0.3646	0.2674	0.1993	0.1624
	1	5	0.7484	0.6640	0.4109	0.2953	0.2185	0.1752
Outer ring	2	1	0.8049	0.6063	0.3937	0.2891	0.2121	0.1677
	2	2	0.8204	0.5579	0.3696	0.2788	0.2213	0.1862
	2	3	0.7964	0.6387	0.4171	0.3101	0.2303	0.1814
	2	4	0.8118	0.6892	0.4554	0.3111	0.2659	0.1988
	2	5	0.8131	0.5760	0.3771	0.2931	0.2178	0.1765
Ball	3	1	0.8398	0.5654	0.3797	0.2731	0.1975	0.1539
	3	2	0.8119	0.5361	0.3678	0.2711	0.1963	0.1565
	3	3	0.8337	0.5878	0.4060	0.2976	0.2080	0.1708
	3	4	0.8205	0.5261	0.3880	0.2959	0.2024	0.1636
	3	5	0.8170	0.5541	0.3793	0.2718	0.2028	0.1592

TABLE 7: Permutation entropy at 1772 rpm.

Fault location	Fault mark	Feature number	Permutation entropy at 1772 rpm					
			PE_1	PE_2	PE_3	PE_4	PE_5	PE_6
Inner ring	1	1	0.7494	0.5420	0.3565	0.2719	0.2092	0.1665
	1	2	0.7520	0.5614	0.3637	0.2730	0.2116	0.1713
	1	3	0.7358	0.6310	0.4070	0.3040	0.2162	0.1721
	1	4	0.7491	0.5292	0.3607	0.2702	0.1970	0.1586
	1	5	0.7446	0.5489	0.3622	0.2706	0.1932	0.1484
Outer ring	2	1	0.8194	0.5606	0.3798	0.2768	0.2112	0.1703
	2	2	0.8142	0.5732	0.3699	0.2895	0.2287	0.1879
	2	3	0.8070	0.5617	0.3677	0.2900	0.2190	0.1872
	2	4	0.8110	0.6117	0.3783	0.2881	0.2200	0.1715
	2	5	0.8144	0.5566	0.3699	0.2923	0.2293	0.1748
Ball	3	1	0.7992	0.5848	0.3893	0.2789	0.2013	0.1545
	3	2	0.8085	0.5766	0.3903	0.2843	0.2063	0.1627
	3	3	0.7860	0.6197	0.4063	0.2842	0.2023	0.1617
	3	4	0.7733	0.5771	0.3853	0.2831	0.2027	0.1580
	3	5	0.7840	0.5785	0.3933	0.2865	0.2106	0.1746

TABLE 8: Permutation entropy at 1792 rpm.

Fault location	Fault mark	Feature number	Permutation entropy at 1792 rpm					
			PE_1	PE_2	PE_3	PE_4	PE_5	PE_6
Inner ring	1	1	0.7363	0.5393	0.3587	0.2674	0.2076	0.1596
	1	2	0.7416	0.5550	0.3508	0.2664	0.1955	0.1513
	1	3	0.7297	0.5633	0.3662	0.2905	0.2084	0.1606
	1	4	0.7299	0.5537	0.3622	0.2656	0.2065	0.1620
	1	5	0.7298	0.5472	0.3685	0.2662	0.1969	0.1530
Outer ring	2	1	0.8217	0.6730	0.4356	0.3176	0.2488	0.1840
	2	2	0.8146	0.6193	0.4082	0.2942	0.2299	0.1747
	2	3	0.8148	0.5702	0.3795	0.2859	0.2282	0.1812
	2	4	0.8258	0.5848	0.3800	0.2927	0.2262	0.1858
	2	5	0.8124	0.6669	0.4430	0.3417	0.2810	0.2267
Ball	3	1	0.8019	0.5699	0.3901	0.2783	0.1957	0.1637
	3	2	0.8041	0.5877	0.3886	0.2841	0.2191	0.1781
	3	3	0.8053	0.5842	0.4002	0.3021	0.2279	0.1732
	3	4	0.8083	0.5844	0.3758	0.2739	0.1967	0.1690
	3	5	0.8183	0.5894	0.3998	0.2959	0.2115	0.1670

TABLE 9: Accuracy of bearing fault recognition.

Case number	Optimization type	Support vector machine parameters			Average value of classification accuracy
		P_k	c_k	g_k	
1	PSO optimized multiclass SVM + HE [5]				97.75%
2	SVM with parameter optimized by ICD [10]				97.91–100%
3	Improved PSO + LS-SVM [14]				89.50%
4	The proposed theory	0.5975	8.3853	50.2970	99.72%

The expression of accuracy is the ratio of the number of correctly classified sets to all sets (including the number of correctly classified sets and the number of incorrectly classified sets).

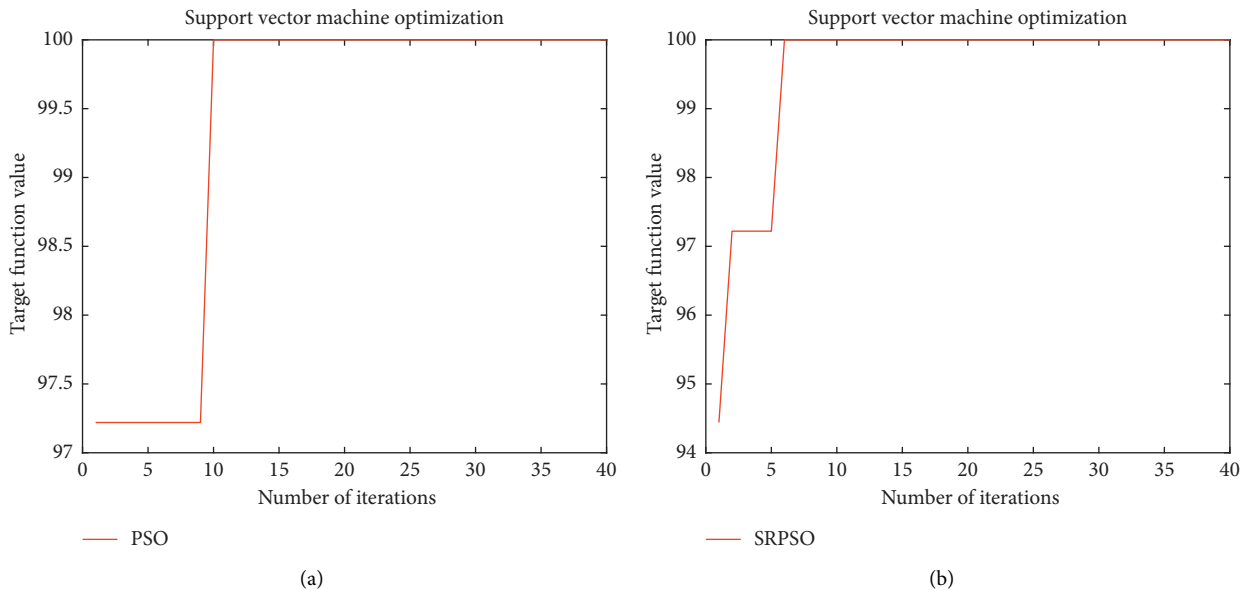


FIGURE 7: (a) PSO optimization training for multikernel single feature LSSVM. (b) SRPSO optimization training for multikernel single feature LSSVM.

third group is IPSO-LSSVM. The proposed method is shown in group 4 [14].

Classification accuracy refers to the ratio of the number of correct classifications to the total samples. As can be seen

from Table 9, the average classification accuracy of the SRPSO optimized MK-LSSVM proposed in this paper is 99.72%. It can be seen that the fault defect classification accuracy of SRPSO optimized MK-LSSVM is higher. The

average recognition accuracy of type 1 is 97.75%. The average recognition accuracy of type 2 is 97.91–100%. Type 3 shows that the recognition accuracy of improved PSO optimized support vector machine under a single feature is 89.50%. The experimental results show that this method can improve the recognition accuracy of rolling bearing by SVM. Comprehensively, SRPSO optimized MK-LSSVM can extract the information of the signal.

5. Conclusions

Based on the analysis of the existing fault diagnosis methods, this paper proposes a SRPSO optimized MK-LSSVM. In this paper, the selection of support vector machine and the feature fusion of signal are given, and the parameters of MK-LSSVM are optimized by SRPSO. The actual results show that the integration of fault feature vectors can improve the adaptability of support vector machines. The optimized MK-LSSVM can obtain more intrinsic information in the signal through the SRPSO theory. Obviously, it has been improved that the classification accuracy was calculated by SRPSO optimized MK-LSSVM.

Data Availability

As for the data, it is put forward by the authors' laboratory experiment table, which is a confidential data, so the authors are sorry for not being able to disclose the data.

Conflicts of Interest

The authors declare that they have no conflicts of interest.

Acknowledgments

This research was supported by the National Natural Science Foundation of China (51565046, 51965052, and 51865045) and Science and Technology Plan Project of Inner Mongolia Autonomous Region, China (KJJH007).

References

- [1] J. Zheng, "Rolling bearing fault diagnosis based on partially ensemble empirical mode decomposition and variable predictive model-based class discrimination," *Archives of Civil and Mechanical Engineering*, vol. 16, no. 4, pp. 784–794, 2016.
- [2] J. Zheng, H. Pan, and J. Cheng, "Rolling bearing fault detection and diagnosis based on composite multiscale fuzzy entropy and ensemble support vector machines," *Mechanical Systems and Signal Processing*, vol. 85, pp. 746–759, 2017.
- [3] D. Dou and S. Zhou, "Comparison of four direct classification methods for intelligent fault diagnosis of rotating machinery," *Applied Soft Computing*, vol. 46, pp. 459–468, 2016.
- [4] F. Chen, B. Tang, T. Song, and L. Li, "Multi-fault diagnosis study on roller bearing based on multi-kernel support vector machine with chaotic particle swarm optimization," *Measurement*, vol. 47, pp. 576–590, 2014.
- [5] K. Zhu, X. Song, and D. Xue, "A roller bearing fault diagnosis method based on hierarchical entropy and support vector machine with particle swarm optimization algorithm," *Measurement*, vol. 47, pp. 669–675, 2014.
- [6] D. Xiang and J. Cen, "Method of roller bearing fault diagnosis based on feature fusion of EMD entropy," *Journal of Aerospace Power*, vol. 30, no. 5, pp. 1149–1155, 2015.
- [7] K. Yu, J. Tan, and L. Shan, "Rolling bearing fault diagnosis research based on multi-sensor information fusion," *Instrument Technique and Sensor*, vol. 7, pp. 97–102, 2016.
- [8] J. A. K. Suykens, T. V. Gestel, J. D. Brabanter, B. D. Moor, and J. Vandewalle, *Least Squares Support Vector Machines*, World Scientific, Singapore, 2002.
- [9] X. Zhang, Y. Liang, J. Zhou, and Y. zang, "A novel bearing fault diagnosis model integrated permutation entropy, ensemble empirical mode decomposition and optimized SVM," *Measurement*, vol. 69, pp. 164–179, 2015.
- [10] Y. Zhang, B. Tang, and P. Xiong, "Rolling element bearing life prediction based on multi-scale mutation particle swarm optimized multi-kernel least square support vector machine," *Chinese Journal of Scientific Instrument*, vol. 37, no. 11, pp. 2489–2496, 2016.
- [11] Y. Lv, F. Hong, T. Yang, F. Fang, and J. Liu, "A dynamic model for the bed temperature prediction of circulating fluidized bed boilers based on least squares support vector machine with real operational data," *Energy*, vol. 124, pp. 284–294, 2017.
- [12] C. Rajeswari, B. Sathiyabhama, S. Devendiran, and K. Manivannan, "Bearing fault diagnosis using wavelet packet transform, hybrid PSO and support vector machine," *Procedia Engineering*, vol. 97, pp. 1772–1783, 2014.
- [13] S. M. H. Bamakan, H. Wang, and A. Zare Ravasan, "Parameters optimization for nonparallel support vector machine by particle swarm optimization," *Procedia Computer Science*, vol. 91, pp. 482–491, 2016.
- [14] W. Deng, R. Yao, H. Zhao, X. Yang, and G. Li, "A novel intelligent diagnosis method using optimal LS-SVM with improved PSO algorithm," *Soft Computing*, vol. 23, no. 7, pp. 2445–2462, 2019.
- [15] J. A. K. Suykens, J. De Brabanter, L. Lukas, and J. Vandewalle, "Weighted least squares support vector machines: robustness and sparse approximation," *Neurocomputing*, vol. 48, no. 1–4, pp. 85–105, 2002.
- [16] C. Wang, X. Wang, C. Zhang, and Z. Xia, "Geometric correction based color image watermarking using fuzzy least squares support vector machine and Bessel K form distribution," *Signal Processing*, vol. 134, pp. 197–208, 2017.
- [17] R. Yan, Y. Liu, and R. X. Gao, "Permutation entropy: a nonlinear statistical measure for status characterization of rotary machines," *Mechanical Systems and Signal Processing*, vol. 29, pp. 474–484, 2012.
- [18] C. Zhang, J. Chen, and X. Guo, "A gear fault diagnosis method based on EMD energy entropy and SVM," *Journal of Vibration and Shock*, vol. 29, no. 10, pp. 216–220, 2010.
- [19] Z. Feng, M. Liang, and F. Chu, "Recent advances in time-frequency analysis methods for machinery fault diagnosis: a review with application examples," *Mechanical Systems and Signal Processing*, vol. 38, no. 1, pp. 165–205, 2013.
- [20] J. Kennedy and R. C. Eberhart, "Particle swarm optimization," in *Proceedings of the IEEE International Conference on Neural Networks*, pp. 1942–1948, IEEE, Piscataway, NJ, USA, 1995.
- [21] M. R. Tanweer, S. Suresh, and N. Sundararajan, "Self regulating particle swarm optimization algorithm," *Information Sciences*, vol. 294, pp. 182–202, 2015.
- [22] Bearing Data Center, Case Western Reserve University, <http://csegroups.case.edu/bearingdatacenter/pages/download-data-file>.